International Journal of Mechanical, Industrial and Aerospace Sciences
ISSN: 2517-9950
Vol:9, No:6, 2015

Stress and Strain Analysis of Notched Bodies Subject to Non-Proportional Loadings

A. Ince

***Abstract*—**In this paper, an analytical simplified method for calculating elasto-plastic stresses strains of notched bodies subject to non-proportional loading paths is discussed. The method was based on the Neuber notch correction, which relates the incremental elastic and elastic-plastic strain energy densities at the notch root and the material constitutive relationship. The validity of the method was presented by comparing computed results of the proposed model against finite element numerical data of notched shaft. The comparison showed that the model estimated notch-root elasto-plastic stresses strains with good accuracy using linear-elastic stresses. The prosed model provides more efficient and simple analysis method preferable to expensive experimental component tests and more complex and time consuming incremental non-linear FE analysis. The model is particularly suitable to perform fatigue life and fatigue damage estimates of notched components subjected to non-proportional loading paths.

***Keywords*—**Elasto-plastic, stress-strain, notch analysis, nonprortional loadings, cyclic plasticity, fatigue.

I. Introduction

NOTCHES and other geometrical irregularities cause stress concentrations in many engineering components. A stress increase induced by stress concentrations stresses results often in localized plastic deformation, leading to fatigue failure. Therefore, the fatigue and durability estimations of notched components require detail knowledge of notch-root stresses and strains [3], [14], [15]. The stress state in the notch root region is in most cases multiaxial in nature. Axles and shafts may experience, for example, combined complex bending and torsion loads. Although Finite Element (FE) commercial software packages can be used to determine notch root stresses and strains in elastic and elastic plastic bodies with a high accuracy for short loading histories such methods are still impractical in the case of long loading histories experienced by machines in service. Therefore non-linear finite element analysis of a long load history would require prohibitively long computing time. For this reason more efficient methods of elastic-plastic stress analysis are needed for widely used engineering applications. One such a method, suitable for calculating multiaxial elastic-plastic stresses and strains in notched bodies subjected to proportional and non-proportional loading histories, is proposed in this paper.

In early researches, elasticity theory or photoelastic analysis was used to determine theoretical stress concentration factors. Neuber [1] proposed the most well-known notch correction method Neuber's rule states that the total strain energy density at the notch equals to the fictitious strain energy density as if a material hypothetically behaved elastic. Molski and Glinka [2] proposed the equivalent strain energy density (ESED) method. The ESED method states that the strain energy density at a notch is equal as if a body hypothetically behaved elastic. Similar approaches were proposed by [4]-[6]. All methods consist of two parts namely the constitutive equations and the notch correction relating the pseudo linear elastic stress-strain state at the notch root with the actual elastic-plastic stress-strain response. Recent notch correction studies [7]–[10] have been conducted to show that the integration of notch correction method(s) and the material constitutive model can be used to calculate the actual elastic-plastic strains and stresses.

The simplified multiaxial stress-strain notch analysis method is developed here to show that the proposed model is efficient and accurate by the comparing computed local stress-strain responses with ANSYS non-linear FE results. Simplified analytical models are preferred due to the simplicity, computational efficiency and low cost as compared to complex and long computing time of the finite element methods.

A. Ince is with the School of Engineering Technology, Purdue University, West Lafayette, IN 47906 USA (phone: 765-494-7519; e-mail: aince@purdue.edu).

II. Stress-Strain State at Notch Root

For the case of general multiaxial loading applied to a notched body, the state of stress near the notch root is tri-axial. However, the stress state at the notch root is bi-axial because of the notch-root stress for a free surface as shown in Fig. 1. Since equilibrium of the infinitesimal element at the notch root must be maintained, i.e. $\sigma^e_{23}=\sigma^e_{32}$ and $\varepsilon^e_{23}=\varepsilon^e_{32}$, there are three non-zero stress components and four non-zero strain components. Seven fictitious linear elastic stress and strain components $(\sigma^e_{ij},\varepsilon^e_{ij})$ can be obtained from the linear elastic solution; however the actual elastic-plastic stress and strain components $(\sigma^a_{ij},\varepsilon^a_{ij})$ at the notch root are unknown. Therefore there are seven unknowns all together and a set of seven independent equations is required for the determination of all actual elasto-plastic stress and strain components at the notch root.

$$\sigma^e_{ij}=\begin{bmatrix}0 & 0 & 0\\ 0 & \sigma^e_{22} & \sigma^e_{23}\\ 0 & \sigma^e_{32} & \sigma^e_{33}\end{bmatrix}\qquad \varepsilon^e_{ij}=\begin{bmatrix}\varepsilon^e_{11} & 0 & 0\\ 0 & \varepsilon^e_{22} & \varepsilon^e_{23}\\ 0 & \varepsilon^e_{32} & \varepsilon^e_{33}\end{bmatrix} \tag{1}$$

The material constitutive relationships provide four equations and remaining three equations can be obtained from the incremental form of the original Neuber rule.

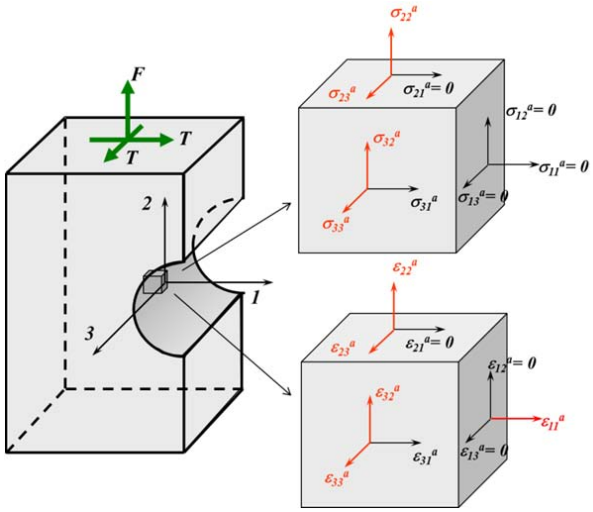

Fig. 1 Stress and strain state at a notch root

III. Material Constitutive Model

The Prandtl-Reuss relation [11], [12], [13] is considered one of the most frequently used models in the incremental plasticity. The total strain increment can be expressed in the form of the Prandtl-Reuss strain-stress relationship.

$$\Delta\varepsilon_{ij}^a = \frac{1+\nu}{E}\Delta\sigma_{ij}^a - \frac{\nu}{E}\Delta\sigma_{kk}^a\,\delta_{ij} + \frac{3}{2}\frac{\Delta\varepsilon_{eq}^{pa}}{\sigma_{eq}^a}\cdot S_{ij}^a \tag{2}$$

The actual deviatoric stress components in the notch root can analogously be defined as:

$$\begin{aligned} S_{ij}^a &= \sigma_{ij}^a - \frac{1}{3}\sigma_{kk}^a\,\delta_{ij} \\ \sigma_{kk}^a &= \sigma_{11}^a + \sigma_{22}^a + \sigma_{33}^a \end{aligned} \tag{5}$$

where σ_{ij}^a are the actual stress components and δ_{ij} is the Kronecker delta. The incremental deviatoric stress-strain relations based on the associated the Prandtl-Reuss flow rule can be subsequently written as:

$$\begin{aligned} \Delta e_{11}^a &= \frac{\Delta S_{11}^a}{2G} + d\lambda\cdot S_{11}^a \\ \Delta e_{22}^a &= \frac{\Delta S_{22}^a}{2G} + d\lambda\cdot S_{22}^a \\ \Delta e_{33}^a &= \frac{\Delta S_{33}^a}{2G} + d\lambda\cdot S_{33}^a \\ \Delta e_{23}^a &= \frac{\Delta S_{23}^a}{2G} + d\lambda\cdot S_{23}^a \end{aligned} \tag{6}$$

where:

$$\frac{1}{2G} = \frac{1+\nu}{E}, \quad d\lambda = \frac{3}{2}\frac{\Delta\varepsilon_{eq}^p}{\sigma_{eq}^a}$$

$$\sigma_{eq}^a = \frac{3}{2}S_{ij}^a S_{ij}^a, \quad \Delta\varepsilon_{eq}^p = \frac{df(\sigma_{eq}^a)}{d\sigma_{eq}^a}\Delta\sigma_{eq}^a$$

where $\Delta\varepsilon_{eq}^{pa}$ is the equivalent plastic strain increment, $\Delta\sigma_{eq}^a$ is the equivalent stress increment, where ν is Poisson's ratio, E is elastic modulus, G is shear modulus. The function, $\Delta\varepsilon_{eq}^{pa} = f\left(\Delta\sigma_{eq}^a\right)$, is identical to the plastic strain – stress relationship obtained experimentally from uniaxial tension test Four notch strain increments $(\Delta e_{11}^a, \Delta e_{22}^a, \Delta e_{33}^a, \Delta e_{23}^a)$ and three notch stress increments $(\Delta\sigma_{22}^a, \Delta\sigma_{33}^a, \Delta\sigma_{23}^a)$ in form seven unknowns to be solved.

IV. Neuber Notch Correction Stress-Strain Relation

The Neuber rule [4] can be written for the uniaxial and multiaxial stress state in the form of (7) and (8) respectively.

$$\sigma_{22}^e\varepsilon_{22}^e = \sigma_{22}^a\varepsilon_{22}^a \tag{7}$$

$$\sigma_{ij}^e\varepsilon_{ij}^e = \sigma_{ij}^a\varepsilon_{ij}^a \tag{8}$$

It should be noted that the original Neuber rule was developed for bodies in pure shear stress state. It means that the Neuber equation states the equivalence of only distortional strain energies. In order to formulate the set of necessary equations for a multiaxial analysis of elastic-plastic stresses and strains at the notch root, the equality of increments of the total distortional strain energy density should be used

Ince et al. [10] proposed to use the equivalence of increments of the total distortional strain energy density contributed by each pair of associated stress and strain components, i.e.,

$$\begin{aligned} S_{22}^e\Delta e_{22}^e + e_{22}^e\Delta S_{22}^e &= S_{22}^a\Delta e_{22}^a + e_{22}^a\Delta S_{22}^a \\ S_{33}^e\Delta e_{33}^e + e_{33}^e\Delta S_{33}^e &= S_{33}^a\Delta e_{33}^a + e_{33}^a\Delta S_{33}^a \\ S_{23}^e\Delta e_{23}^e + e_{23}^e\Delta S_{23}^e &= S_{23}^a\Delta e_{23}^a + e_{23}^a\Delta S_{23}^a \end{aligned} \tag{9}$$

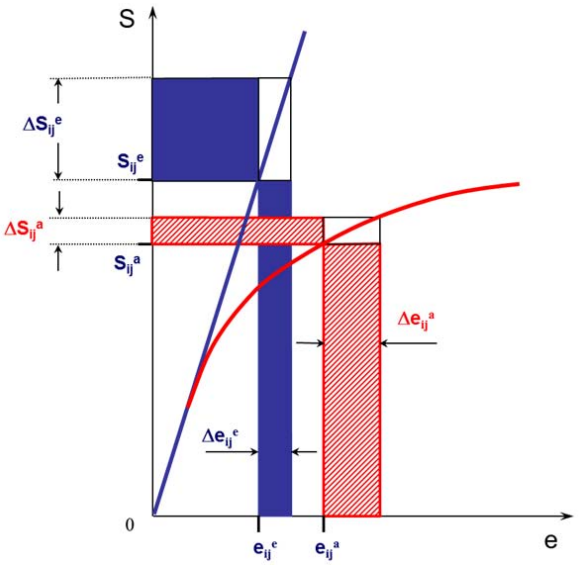

Fig. 2 Graphical representation of the incremental Neuber rule

The equalities of strain energy increments for each set of

corresponding hypothetical elastic and actual elastic-plastic strains and stress increments at the notch root can be shown graphically in Fig. 2. The area of dotted rectangles represents the total strain energy increment of the hypothetical elastic notch root input stresses while the area of the hatched rectangles represents the total strain energy density of the actual elastic-plastic material response at the notch root.

Consequently, a combination of four equations from the elastic–plastic constitutive in (6) and three equations from the equivalence of increments of the total distortional strain energy density in (9) yields the required set of seven independent equations necessary to completely define elastic–plastic notch-root strain and stress responses for a notched component subjected to multiaxial non-proportional loads. The combined set of equations are written as a set of seven simultaneous equations from which all unknown deviatoric strain, Δe_{ij}^{a} and stress, ΔS_{ij}^{a} increments can be calculated.

The calculated deviatoric stress increments, ΔS_{ij}^{a}, can subsequently be converted into the actual stress increments, $\Delta \sigma_{ij}^{a}$ using (10):

$$\begin{aligned}\Delta S_{22}^{a} &= \Delta\sigma_{22}^{a} - \frac{1}{3}\left(\Delta\sigma_{22}^{a} + \Delta\sigma_{33}^{a}\right) \\ \Delta S_{33}^{a} &= \Delta\sigma_{33}^{a} - \frac{1}{3}\left(\Delta\sigma_{22}^{a} + \Delta\sigma_{33}^{a}\right) \\ \Delta S_{23}^{a} &= \Delta\sigma_{23}^{a}\end{aligned} \tag{10}$$

V. Results and Discussion

The set of data was obtained for multiaxial non-proportional load paths in order to verify the prediction accuracy of the proposed method. For that purpose several non-linear Finite Element analyses have been carried out using two different load paths.

For non-proportional stress paths, the accuracy of the method was demonstrated by comparing the calculated notch root stress-strain responses to those obtained from the finite element method. The elastic-plastic finite element stress results were obtained using the ANSYS finite element software. The isotropic strain-hardening plasticity model was used for calculations. The geometry of the notched element was that of the circumferentially notched bar shown in Fig. 7.

The basic proportions of the cylindrical notched bar were $\rho/t = 1$ and $R/t = 2$ resulting in the tensile and torsion stress concentration factor $K_F = 1.41$ and $K_T = 1.15$ respectively. The ratio of the notch root hoop stress to the axial stress under tensile axial loading was $\sigma_{33}^{e}/\sigma_{22}^{e} = 0.184$. The actual radius of the cylindrical specimen was R=25.4 mm. The material for the notched bar was SAE 1070 steel with a cyclic stress-strain curve approximated by the Ramberg- Osgood relation in (11). The material properties were: E = 210 GPa, $\nu = 0.3$, $S_Y = 242$ MPa, n'=0.199, and K' = 1736 MPa.

$$\varepsilon = \frac{\sigma}{E} + \left(\frac{\sigma}{K'}\right)^{\frac{1}{n'}} \tag{11}$$

while the nominal stresses in the net cross section were determined as:

$$\sigma_n = \frac{P}{\pi\left(R-t\right)^2} \quad \text{and} \quad \tau_n = \frac{T}{\pi\left(R-t\right)^3} \tag{12}$$

The first load path applied to the notched bar were monotonically increasing torsion in the first phase and then increasing tension in the second phase while the torsion load being kept constant as shown in Fig. 3. The torque T induced the 'linear elastic' shear stress σ_{23}^{e} at the notch root and the axial load F induced the normal stress components σ_{22}^{e} and σ_{33}^{e}. The increments of the hypothetical 'elastic" stress components σ_{23}^{e}, σ_{22}^{e} and σ_{33}^{e} and associated strains were used as the input to the model. The pseudo elastic equivalent stress of the input at the notch root was increasing throughout the entire loading process to ensure monotonic loading path.

The computed stress and strain responses from the analytical proposed model were compared with the elasto-plastic stress-strain components obtained from the non-linear FE analysis in in Figs. 4, and 5. Fig. 4 shows the computed and FE determined stress components, σ_{22}^{a} and σ_{23}^{a} and Fig. 5 shows the computed and the FE model determined strain components, ε_{22}^{a} and ε_{23}^{a}. Note, that the calculated stress and strain responses and the results of the finite element analysis are identical in the elastic range. This is expected since the model converges to the elastic solution in the elastic range. However, beyond the yield point at the notch root, the stress and strain results that were predicted using the proposed model and the finite element data begin gradually to diverge. As seen from Figs. 4 and 5 that the model slightly underestimates the actual notch root shear stresses and strains for the first load path but the predicted stresses and strains are very close to the numerical FE data.

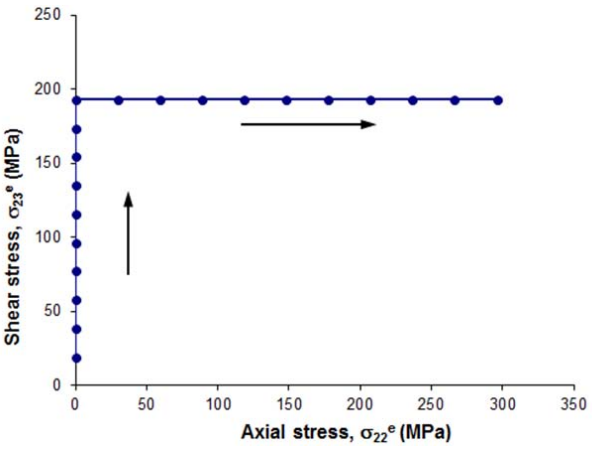

Fig. 3 The non-proportion torsion-tension load path

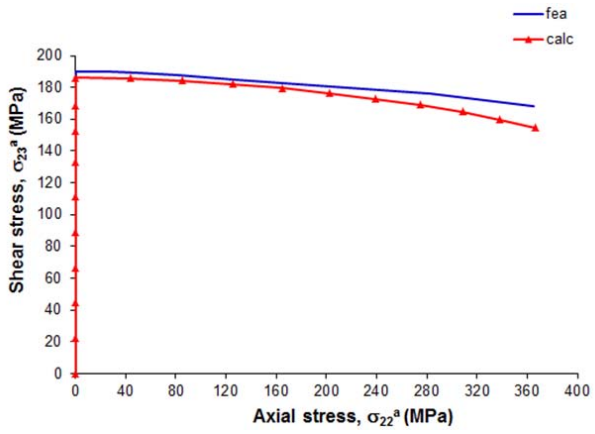

Fig. 4 Comparison of the calculated and FEM determined stress paths for the non-proportional torsion-tension load path

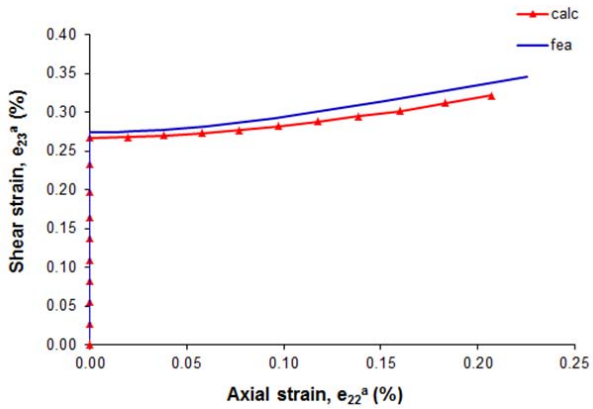

Fig. 5 Comparison of the calculated and FEM determined strain paths for the non-proportional torsion-tension load path

The second load path applied to the notched bar were monotonically increasing tension in the first phase and then increasing torsion in the second phase while the tension load being kept constant as shown in Fig. 6. The axial load F induced the 'linear elastic' normal stress components σ_{22}^e and σ_{33}^e and the torque T induced the 'linear elastic' shear stress σ_{23}^e at the notch root. The increments of the hypothetical 'elastic" stress components σ_{23}^e, σ_{22}^e and σ_{33}^e and associated strains were used as the input to the model. The pseudo elastic equivalent stress of the input at the notch root was increasing throughout the entire loading process to ensure monotonic loading path.

The computed stress responses and the stress responses from the non-linear FE analysis are compared in Fig. 7. Similarly, the computed strain responses and the non-linear FE strain responses are compared in Fig. 8. As expected, the calculated stresses and strains and the results of the finite element analysis are same in the elastic range. However, after yielding at the notch root, the strain results that were predicted using the proposed model and the finite element data begin gradually to diverge. Figs. 7 and 8 show that the model slightly underestimates the actual notch root axial stresses and strains for the second load path but the predicted stresses and strains are in good agreement with the numerical FE data.

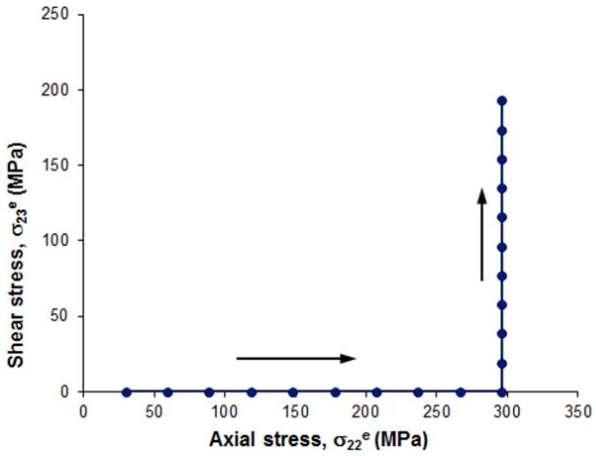

Fig. 6 The non-proportion tension-torsion load path

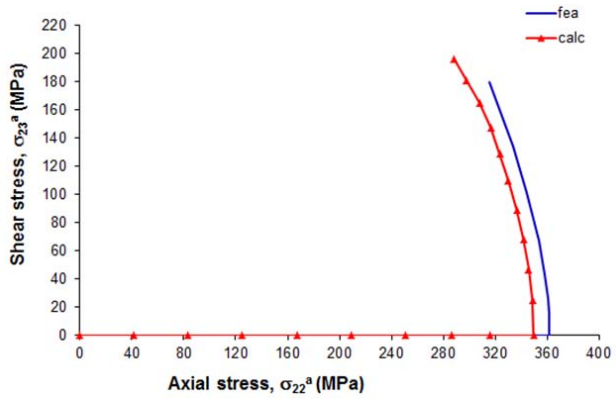

Fig. 7 Comparison of the calculated and FEM determined stress paths for the non-proportional tension- torsion load path

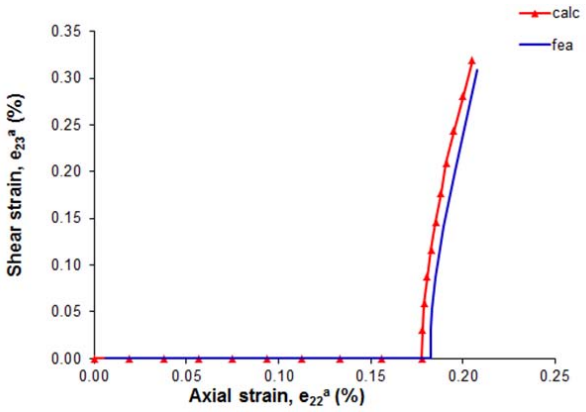

Fig. 8 Comparison of the calculated and FEM determined strain paths for the non-proportional torsion-tension load path

VI. Conclusion

In this paper, the simple and efficient analytical method for calculating elasto-plastic notch root streses and strains induced

by multiaxial non-proportional load paths has been proposed. The method has been formulated using with the material constitutive relation and the increments of the total strain energy density based on the Neuber correction rule. The proposed model has been validated with finite element data obtained for two non-proportional loading paths. Based on the comparison between numerical data from the non-linear FE analysis and calculated stress and strain responses from the model for two different non-proportional load paths, the simplified model calculated notch stresses strains with reasonable accuracy using linear-elastic stresses.

The proposed model provides a more efficient and simple analytical approach to calculate notch root elastic-plastic stresses and strains for the notch component under the multiaxial non-proportional loadings. The calculated notch root stresses and strains can be subsequently used to perform fatigue life estimations for the notched components subject to complex multiaxial loadings.

REFERENCES

[1] Neuber, H., Theory of Stress Concentration for Shear Strained Prismatic Bodies with Arbitrary Stress–Strain Law, Journal of Appl. Mechanics, Vol. 28, pp. 544-550, 1961.

[2] Molski, K., Glinka, G., A Method of Elastic-Plastic Stress and Strain Calculation at a Notch Root, Materials Science and Engineering, Vol. 50, pp. 93- 100, 1981.

[3] Ince, A. and Glinka, G., A Generalized Damage Parameter for Multiaxial Fatigue Life Prediction under Proportional and Non-Proportional Loadings, International Journal of Fatigue, Vol.62, pp. 34-41, 2014.

[4] Hoffmann, M., Seeger, T., A Generalized Method for Estimating Multiaxial Elastic–Plastic Notch Stresses and Strains, Part I: Theory, Journal of Engineering Materials and Technology, Vol. 107, pp. 250-254, 1985.

[5] Moftakhar, A., Buczynski, A. and Glinka, G., "Calculation of Elasto-Plastic Strains and Stresses in Notches under Multiaxial Loading", International Journal of Fracture, Vol.70, pp. 357-373, 1995.

[6] Singh, M.N.K., Notch Tip Stress-Strain Analysis in Bodies Subjected to Non-Proportional Cyclic Loads, Ph.D. Dissertation, Dept. Mech. Eng., University of Waterloo, Ontario, Canada, 1998.

[7] Buczynski, A., and Glinka, G., Elastic-plastic Stress-Strain Analysis of Notches under Non-Proportional Loading Paths, in Proceedings of the International Conference on Progress in Mechanical Behaviour of Materials (ICM8), Victoria, May 16-21, 1999, eds. F. Ellyin and J.W. Provan, 3, pp. 1124-1130, 1999.

[8] Koettgen, V.B., Barkey, M.E., Socie, D.F., Pseudo Stress and Pseudo Strain Based Approaches to Multiaxial Notch Analysis, Fatigue of Engineering Materials and Structures 34, pp.854–867, 2001.

[9] Ince, A. and Glinka, G., A Numerical Method for Elasto-Plastic Notch-Root Stress-Strain Analysis, Journal of Strain Analysis for Engineering Design, Vol. 48, No. 4, pp. 229-224, 2013.

[10] Ince, A., Glinka, G. and Buczynski, A., A Computational Modeling Technique of Elasto-Plastic Stress-Strain Response for Notched Components, International Journal of Fatigue, Vol.62, pp. 42-52, 2014.

[11] Garud, Y.S., A New Approach to the Evaluation of Fatigue under Multiaxial Loadings, Journal of Engineering Materials and Technology, 103, pp. 118- 125, 1981.

[12] Prandtl, W., Spannungsverteilung in Plastischen Kerpern, Proceedings of the First International Congress on Applied Mechancis, pp. 43, 1924.

[13] Reuss, E., Beruecksichtigung der elastischen Formaenderungen in der Zeit- schrift fur Angewandte Mathematik und Mechanik, Vol. 10, pp. 266-274, 1930.

[14] Ince, A. and Glinka, G., "Innovative Computational Modeling of Multiaxial Fatigue Analysis for Notched Components", International Journal of Fatigue, 2015, doi:10.1016/j.ijfatigue.2015.03.019

[15] Ince, A., "A novel technique for multiaxial fatigue modelling of ground vehicle notched components", International Journal of Vehicle Design, Vol. 67, No.3, pp. 294-313, 2015, doi: 10.1504/IJVD.2015.069486.